Structure and thermal characteristics of the summit dome, March, 1990 - March, 1991: Volcán Colima, Mexico

Charles B. Connor[1], Sammantha B. Lane and Bradford M. Clement
Dept. of Geology, Florida International University, Miami, USA.
[1] *Current address: Center for Nuclear Waste Regulatory Analyses, Southwest Research Institute, San Antonio, Texas, USA.*

RESUMEN

Un nuevo lóbulo de lava fue extrusionado sobre el domo del Volcán de Colima a principio de marzo, 1991. En el primer día de actividad eruptiva, el nuevo lóbulo del domo creció a un volumen aproximado de 2,200 m^3 de forma circular con diámetro de alrededor de 20 m y altura de aproximadamente 6.5 m. Alrededor del lóbulo del domo se formó una depresión somera con intensa desgasificación. Se observaron fracturas radiales que se extendían a partir del lóbulo del domo indicando que el esfuerzo horizontal conpresivo principal estaba orientado radialmente al domo durante la extrusión. El fallamiento más prominente resultó en la formación de un pequeño graben, de aproximadamente 20 m de ancho y bordeado por escarpes con 3 a 5 m de desplazamiento vertical extendíendose hacia el NNW del nuevo lóbulo del domo.

Observaciones geofísicas hechas sobre el domo en 1990 indican que la extrusión inicial del nuevo lobulo estuvo controlada por una estructura preexistente. El lóbulo del domo se extrusionó aproximadamente 30 m al sur de la única fumarola de alta temperatura (350-375°) que se encontraba sobre el domo en 1990. Cuatro fumarolas monitoreadas durante marzo, mayo y diciembre 1990, se desgasificaron en estado constante en 1990 con flujos de masa bajos. Hubo poco cambio en la media de las temperaturas de las fumarolas. Las observaciones magnéticas terrestres obtenidas en diciembre de 1990 en un transecto sobre el campo de las fumarolas muestran una anomalía magnética de longitud de onda corta, 2000 nT, centrada en el campo de las fumarolas. Las rocas del domo muestran suceptibilidades magnéticas comparativamente bajas (8.42x10^{-6}-8.06x10^{-5} corregido por masa SI) y magnetizaciones remanentes altas (1.08-5.57 A/m). Nuestro modelo de los datos magnéticos, incorporando estas observaciones del magnetismo de las rocas, indica que la fuente de la anomalía magnética fue un cuerpo pequeño y somero de roca que fue calentada por los gases fumarólicos por encima de las temperatura de bloqueo NRM de las rocas del domo. Este cuerpo de roca caliente era alargado en dirección NNW y coincide exactamente con el escape oriental del graben formado durante la extrusión inicial del lóbulo de lava de marzo, 1991. La aplicación de un modelo numérico de transferencia de calor y de masa sugiere que las fumarolas que se desgasifiquen en un estado constante y con flujo de masa bajo en un magma somero empobrecido en volatíles crearán una anomalía térmica similar a la que se deduce en el módulo magnético. Los derrames de roca sobre las partes altas del Volcán son más intensos sobre las extensiones norte y sur del nuevo graben. La coincidencia de los rasgos estructurales y térmicos sugiere que el graben con orientación NNW que se formó durante la actividad de 1991 es una manifestación superficial de una estructura mayor que corta la parte superior del Volcán y sobre la cual puede ocurrir deformación adicional en el futuro.

PALABRAS CLAVE: Domo, temperatura, fumarolas, magnetismo, graben.

ABSTRACT

A new exogeneous dome lobe erupted on the summit lava dome of Volcán de Colima, Mexico, early in March, 1991. Within the first day of eruptive activity the new dome lobe grew to a volume of approximately 2,200 m^3, was circular in shape, had a diameter of about 20 m and a height of approximately 6.5 m. This dome lobe was surrounded by a shallow moat, from which degassing was intense. Radial fractures extended from the dome lobe, indicating that principal horizontal compressional stresses were oriented radial to the dome at the time of extrusion. The most prominent faulting resulted in the formation of a small graben, approximately 20 m in width and bounded by scarps with 3 m to 5 m of vertical displacement, extending NNW of the new dome lobe.

Geophysical observations made on the summit lava dome throughout 1990 indicate that the initial extrusion of this dome lobe was controlled by a pre-existing structure. The dome lobe extruded approximately 30 m south of the only high-temperature (350-575°C) fumarole field occurring on the summit dome during 1990. Four fumaroles monitored during March, May and December, 1990, degassed in a steady-state from this field throughout 1990 at low mass flows. Little change in mean fumarole temperatures occurred during this period. Ground magnetic observations collected in December, 1990, along a traverse across this high-temperature fumarole field reveal a short-wavelength, -2000nT magnetic anomaly, nearly centered on the fumarole field. Summit dome rocks have comparatively low magnetic susceptibilities (8.42x10^{-6}-8.06x10^{-5} mass-corrected SI) and high remanent magnetizations (1.08-5.57 A/m). Our model of the magnetic data, incorporating these rock magnetic observations, indicates that the source of the magnetic anomaly was a small, shallow body of rock which was heated by the ascending fumarole gases to above the NRM unblocking temperatures of summit dome rocks. This body of hot rock was elongated in a NNW direction and coincides exactly with the eastern scarp of the graben formed during the initial extrusion of the March, 1991 dome lobe. Application of a numerical heat and mass transfer model suggests that fumaroles degassing in a steady-state and low mass flow from a shallow, volatile-depleted magma, will create a thermal anomaly similar to that deduced from the magnetic model. Rock-avalanching from high on the flanks of the volcano is also most intense along the northern and southern extensions of the new graben. The coincidence of these structural and thermal features suggests that the NNW-trending graben formed during 1991 activity is the surface manifestation of a major structure transecting the upper edifice of the volcano, along which additional deformation may occur in the future.

KEY WORDS: Dome, temperature, fumarole field, magnetism, graben.

INTRODUCTION

On March 1, 1991, a new lobe was observed actively extruding on the summit lava dome of Volcán Colima, Mexico (19.51°N, 103.61°W) (Figure 1). This eruption, which later resulted in a lava flow on the south flank of the volcano as the dome grew, was the first extrusive activity to occur at Colima since the effusion of lava flows in 1981-1982 (McClelland *et al.*, 1989). In addition to the extrusion of juvenile material, the eruption has resulted in tremendous deformation of the summit area of the volcano and numerous rock avalanches on its flanks. Our purpose is to describe this deformation in light of direct observations made on the summit dome during 1990 and following the onset of extrusive activity early in March, 1991. Detailed descriptions of subsequent events are available elsewhere (GVN, 1991; Rodríguez-Elizarrarás *et al.*, 1991).

Data discussed here include fumarole temperature measurements collected continuously for periods of time ranging from 2 days to 25 days in March, May and December, 1990, a limited number of ground magnetic measurements collected during December, 1990, and measurements of the magnetic properties of summit dome rocks. We originally collected these data with the intention of describing long term thermal changes wihin the summit dome. Although this goal is no longer tenable because of the 1991 activity on the dome, these data provide clues to the nature of structural controls on the March, 1991 extrusive activity and possibly future eruptive activity. In addition, we prepared a map of new structural features of the dome using compass and tape methods, and from oblique aerial photos taken in March, 1991. Integrating fumarole temperature measurements, rock magnetic data and field magnetic observations with structural mapping provides a more complete view of stuctural controls of heat and mass transfer on the dome than in otherwise possible. Evaluation of this map in light of observations made on the dome prior to the March eruption provides insights into structure controls on this recent activity.

Details of the eruptive history of Volcán Colima have been presented elsewhere (Luhr, 1981; Medina, 1983; Luhr and Carmichael, 1990; Stoopes, 1991; Martín del Pozzo, 1990; Stoopes and Sheridan,1992). Holocene activity has included several voluminous volcanic debris avalanches (Luhr and Prestegaard, 1988; Stoopes and Sheridan 1992). Since its earliest historial activity in 1560, Colima volcano has evolved through four eruptive cycles, each with a duration of approximately 100 years (Luhr and Carmichael, 1980; 1990). Historical data for the earliest cycles are of relatively poor quality, and these cycles are hypothesized based on analogy with the third (1818-1913) and fourth (1913-present) eruptive cycles. Both the second and the third cycles ended with powerful explosive eruptions that generated ashfalls up to 700 km from the volcano and produced pyroclastic flows on the southern flanks of the volcano, some of which extend 15 km from the summit vent and decimated areas which are presently populated.

STRUCTURE OF THE SUMMIT DOME, 1990

Throughout 1990, the summit area of the volcano remained essentially unchanged. Topography of the summit lava dome was dominated by numerous depressions of variable size formed by explosive phreatic activity, and elevated areas formed from older blocky dome lobes (Figure 1). Small fractures, less than 20 cm in width and of variable lengths and orientations, were distributed across the dome. In some sections of the dome, particularly on its north and northeast sides, these fractures appeared to be preferentially aligned with N30-60E orientations. Gases vented from small fumaroles located along these fractures. No large fractures (widths > 20 cm) or other deformational features appeared to have developed since 1985 (McClelland *et al.*, 1989).

FUMAROLE TEMPERATURES

Fumarole temperatures on the summit dome of the volcano decreased between 1985 and March, 1990 (McClelland *et al*, 1989, GVN, 1990). Areas which were the sites of intense fumarole activity as late as 1987, with jetting fumaroles and temperatures as high as 800°C, were quiescent in 1990. As a result, we were able to easily reach many parts of the dome which had been previously inaccessible. During 1990, low-temperature fumaroles (< 200° C) were widely distributed on the summit dome. High-temperature fumaroles (350-575°C) were only found on the western-central portion of the summit dome (Figure 1). These fumaroles were located in short, discontinuous fractures less than 15 cm wide.

Extensive measurements were made of these high-temperature fumaroles in March, May and December of 1990 (GVN, 1990). During these months we used a Campbell Scientific datalogger to monitor four fumaroles for periods of four, twenty-five, and two days, in March, May and December, respectively. Measurements were made at intervals of between three and twenty minutes. An example of one of the resulting time series, for measurements made in the hottest fumarole in the field during May, is given in Figure 2. Summary statistics for all four fumaroles are given in Table 1. These data illustrate two points about fumarole temperatures on the summit dome during 1990. First, daily fluctuations of 30-60° occurred in most fumaroles accounting for most of the temperature range observed in the fumaroles. These fluctuations likely result from daily barometric pressure variation, which is known to affect degassing rates (Baubron *et al.*, 1991; Connor *et al.*, 1992). Temperature fluctuations of this amplitude will only occur in fumaroles with low mass flows (gas velocities of less than approximately 2 m/s; Connor *et al.*, 1992). Although gas velocities were not measured in these fumaroles, visual observations indicated that gas velocities at the surface were low in all of them during the sampling periods. In order for fumarole temperatures to be maintained at over 500°C in thin fractures with low mass flows, as they were in one fumarole throughout 1990 (Table 1), magma or rocks at near magmatic temperatures must be
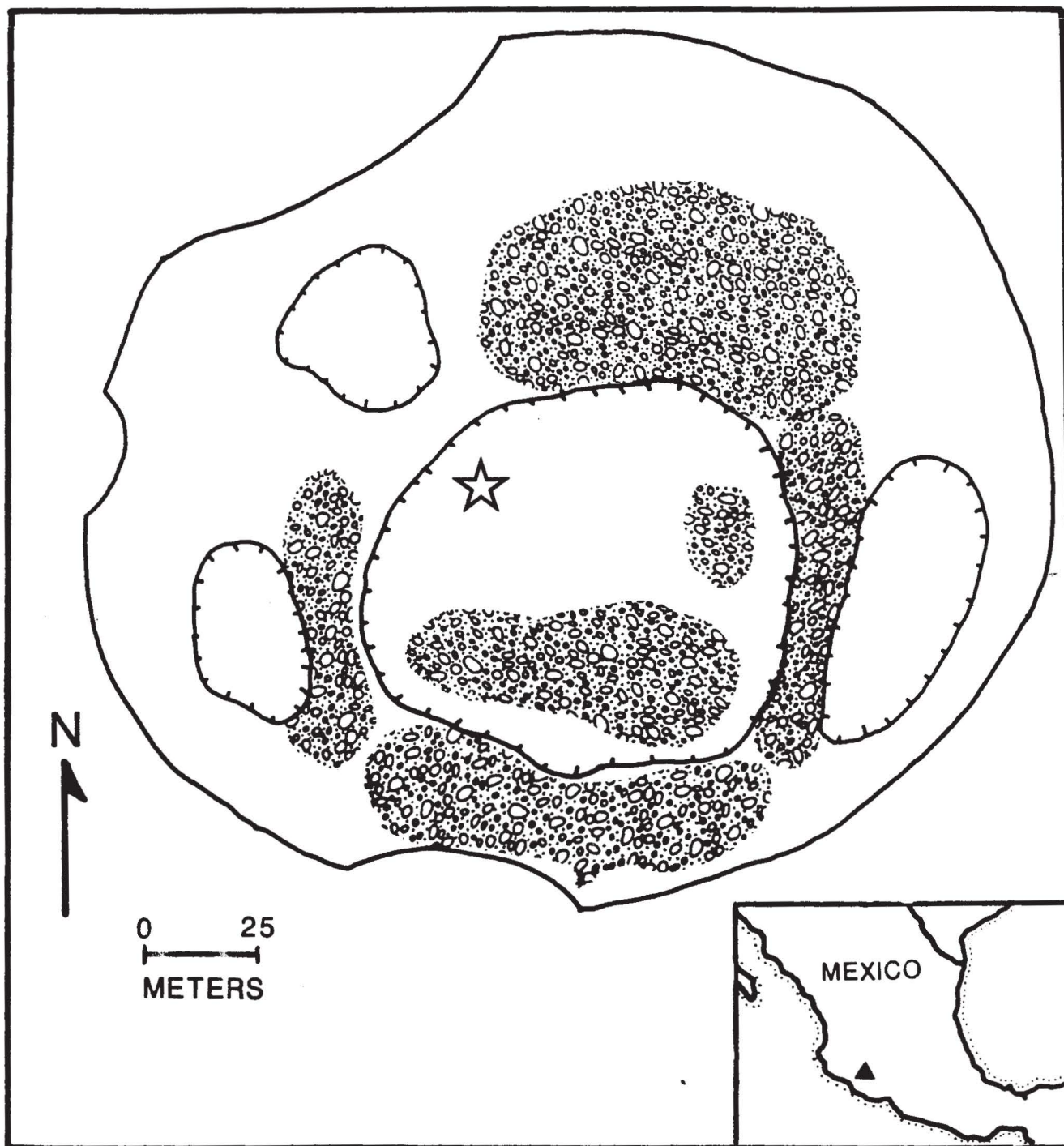
Fig. 1. Summit dome of Volcán Colima, as it appeared in 1990. This map has been modified slightly from one prepared using tape and compass techniques by A. L. Martin, T. Kerdan, L. Vázquez and F. Sainz (GVN, 1990). Topographic depressions on the summit dome (hachured lines) are quite shallow, generally less than 10 m deep. Elevated rubbly dome lobes (pattern) are also of low relief (10-15 m). Although low-temperature fumaroles (< 200°C) were widely scattered on the dome during 1990, high-temperature fumaroles (350°-575°C) were restricted to a limited area on the west-central portion of the dome (star). The topographic edge of the summit dome (solid line) is scalloped by avalanche scars high on the flanks of the volcano, particularly on the western half of dome. Inset: Location of Volcán Colima, Mexico.

located at shallow depth (probably less than 200 m; Connor, 1990; 1992). Second, fumarole temperatures declined slightly between March and May in all three fumaroles monitored (Table 1). Temperatures then rose slightly or remained steady between May and December. By December, the plumbing of the fumarole field had altered and one fumarole had cooled completely (Fumarole #2, Table 1), while several others had appeared (eg: Fu-

INTRODUCTION

On March 1, 1991, a new lobe was observed actively extruding on the summit lava dome of Volcán Colima, Mexico (19.51°N, 103.61°W) (Figure 1). This eruption, which later resulted in a lava flow on the south flank of the volcano as the dome grew, was the first extrusive activity to occur at Colima since the effusion of lava flows in 1981-1982 (McClelland et al., 1989). In addition to the extrusion of juvenile material, the eruption has resulted in tremendous deformation of the summit area of the volcano and numerous rock avalanches on its flanks. Our purpose is to describe this deformation in light of direct observations made on the summit dome during 1990 and following the onset of extrusive activity early in March, 1991. Detailed descriptions of subsequent events are available elsewhere (GVN, 1991; Rodríguez-Elizarrarás et al., 1991).

Data discussed here include fumarole temperature measurements collected continuously for periods of time ranging from 2 days to 25 days in March, May and December, 1990, a limited number of ground magnetic measurements collected during December, 1990, and measurements of the magnetic properties of summit dome rocks. We originally collected these data with the intention of describing long term thermal changes within the summit dome. Although this goal is no longer tenable because of the 1991 activity on the dome, these data provide clues to the nature of structural controls on the March, 1991 extrusive activity and possibly future eruptive activity. In addition, we prepared a map of new structural features of the dome using compass and tape methods, and from oblique aerial photos taken in March, 1991. Integrating fumarole temperature measurements, rock magnetic data and field magnetic observations with structural mapping provides a more complete view of structural controls of heat and mass transfer on the dome than in otherwise possible. Evaluation of this map in light of observations made on the dome prior to the March eruption provides insights into structure controls on this recent activity.

Details of the eruptive history of Volcán Colima have been presented elsewhere (Luhr, 1981; Medina, 1983; Luhr and Carmichael, 1990; Stoopes, 1991; Martín del Pozzo, 1990; Stoopes and Sheridan, 1992). Holocene activity has included several voluminous volcanic debris avalanches (Luhr and Prestegaard, 1988; Stoopes and Sheridan 1992). Since its earliest historial activity in 1560, Colima volcano has evolved through four eruptive cycles, each with a duration of approximately 100 years (Luhr and Carmichael, 1980; 1990). Historical data for the earliest cycles are of relatively poor quality, and these cycles are hypothesized based on analogy with the third (1818-1913) and fourth (1913-present) eruptive cycles. Both the second and the third cycles ended with powerful explosive eruptions that generated ashfalls up to 700 km from the volcano and produced pyroclastic flows on the southern flanks of the volcano, some of which extend 15 km from the summit vent and decimated areas which are presently populated.

STRUCTURE OF THE SUMMIT DOME, 1990

Throughout 1990, the summit area of the volcano remained essentially unchanged. Topography of the summit lava dome was dominated by numerous depressions of variable size formed by explosive phreatic activity, and elevated areas formed from older blocky dome lobes (Figure 1). Small fractures, less than 20 cm in width and of variable lengths and orientations, were distributed across the dome. In some sections of the dome, particularly on its north and northeast sides, these fractures appeared to be preferentially aligned with N30-60E orientations. Gases vented from small fumaroles located along these fractures. No large fractures (widths > 20 cm) or other deformational features appeared to have developed since 1985 (McClelland et al., 1989).

FUMAROLE TEMPERATURES

Fumarole temperatures on the summit dome of the volcano decreased between 1985 and March, 1990 (McClelland et al, 1989, GVN, 1990). Areas which were the sites of intense fumarole activity as late as 1987, with jetting fumaroles and temperatures as high as 800°C, were quiescent in 1990. As a result, we were able to easily reach many parts of the dome which had been previously inaccessible. During 1990, low-temperature fumaroles (< 200° C) were widely distributed on the summit dome. High-temperature fumaroles (350-575°C) were only found on the western-central portion of the summit dome (Figure 1). These fumaroles were located in short, discontinuous fractures less than 15 cm wide.

Extensive measurements were made of these high-temperature fumaroles in March, May and December of 1990 (GVN, 1990). During these months we used a Campbell Scientific datalogger to monitor four fumaroles for periods of four, twenty-five, and two days, in March, May and December, respectively. Measurements were made at intervals of between three and twenty minutes. An example of one of the resulting time series, for measurements made in the hottest fumarole in the field during May, is given in Figure 2. Summary statistics for all four fumaroles are given in Table 1. These data illustrate two points about fumarole temperatures on the summit dome during 1990. First, daily fluctuations of 30-60° occurred in most fumaroles accounting for most of the temperature range observed in the fumaroles. These fluctuations likely result from daily barometric pressure variation, which is known to affect degassing rates (Baubron et al., 1991; Connor et al., 1992). Temperature fluctuations of this amplitude will only occur in fumaroles with low mass flows (gas velocities of less than approximately 2 m/s; Connor et al., 1992). Although gas velocities were not measured in these fumaroles, visual observations indicated that gas velocities at the surface were low in all of them during the sampling periods. In order for fumarole temperatures to be maintained at over 500°C in thin fractures with low mass flows, as they were in one fumarole throughout 1990 (Table 1), magma or rocks at near magmatic temperatures must be

Table 1

	no. of samples	mean (°C)	std. dev. (°C)	max. (°C)	min. (°C)
Fumarole #1					
March	1861	541.8	14.0	570.9	508.9
May	1805	518.2	12.2	560.6	478.8
December	1302	527.8	8.2	540.3	495.3
Fumarole #2					
March	1861	481.3	1.93	486.1	478.3
May	1805	473.7	1.56	477.6	467.0
Fumarole #3					
March	1861	478.3	2.03	483.3	471.0
May	1805	397.8	8.62	414.0	342.1
December	1302	392.5	14.1	418.0	359.6
Fumarole #4					
December	1302	341.4	4.58	356.2	330.1
Surface					
March	1861	28.0	8.3	44.9	12.5
May	1805	33.3	6.9	50.6	15.1
December	1302	12.3	6.3	27.4	6.2

Descriptive statistics for temperature variation monitored in four high-temperature fumaroles on the summit dome of Volcán Colima during 1990. Surface temperatures are also reported for the same period.

is slightly smaller in amplitude and much shorter in wavelength than magnetic anomalies associated with thermal areas on Showa-shinzan dome, Usu volcano, Japan (Nishida and Miyajima, 1984) and the dacite dome of Mount St. Helens (Dzurisin et al., 1990), indicating the anomaly source is a comparatively shallow, localized feature. The close association between the magnetic anomaly and the high temperature fumarole field, however, suggests a thermal origin for the anomaly.

ROCK MAGNETIC PROPERTIES.

As part of a larger study of the rock magnetic properties of lavas extruded from Volcan Colima, we collected six samples from the summit crater and recent flows high on the flanks of the volcano. The samples are andesitic in composition and in varying stages of alteration, although most are quite fresh. Some of the samples are vesicular while others are well indurated.

Because the surface of the summit is covered with large boulders and talus, six unoriented hand samples were collected for rock magnetic study. Twenty-eight specimens were drilled from the hand-samples and subjected to thermal demagnetization and rock magnetic experiments in order to constrain the magnetic characteristics of the summit dome. The magnetizations were measured using a three axis, superconducting, cryogenic magnetometer. Each of the specimens was subjected to progressive thermal demagnetization at 50°C intervals to 550°C and then 10°C intervals from 570-580°C. Bulk magnetic susceptibilities were measured using a Bartington susceptibility meter (model MS2) and corrected for mass. The sus-

ceptibility of each specimen was measured at room temperature prior to each heating stage of the thermal demagnetization to monitor possible changes in the composition of the magnetic carriers as a result of the heating.

The progressive thermal demagnetization experiments revealed nearly univectorial magnetizations in each of the 28 specimens. Although the hand samples were unoriented, the stability of the magnetizations and the uniformity of the magnetization directions observed within each of the blocks suggests that the magnetizations are primary and that these rocks are good magnetic recorders. By extrapolation we infer that indurated portions of flows at the dome are magnetized in the direction of the present-day Earth's magnetic field.

Results of the thermal demagnetization indicate that these rocks exhibit a discrete unblocking temperature spectra (Figure 5). Most specimens retained their NRM intensities up to about 400°C above which the magnetizations began to decrease. In the majority of the samples, 90% of the NRM is unblocked between 450°C and 570° C. These results, together with the isothermal remanent magnetization experiments suggest that magnetite or titanomagnetite is the dominant magnetic carrier in these samples. The observed variability in the demagnetization curves (Figure 5) probably indicates some variation in magnetic mineral content or grain size.

Magnetic susceptibilities range from 8.42×10^{-6} to 8.06×10^{-5}, with a mean of 4.23×10^{-5} (mass-corrected SI). The samples displayed no significant variation after heating, indicating that no major changes in the magnetic carrier occurred during thermal demagnetization. This behavior suggests that heating of lavas around fumaroles is unlikely to produce large chemical remanent magnetization anomalies. Additional experiments indicate that susceptibility variations due to temperature (Hopkinson effect) are small in these rocks (no more than 30% of measured susceptibility). The mean NRM intensity is 3.21 A/m with NRM intensities in individual specimens ranging from 1.08 A/m to 5.57 A/m (Table 2). The NRM intensities are high relative to the magnetic susceptibilities, suggesting that magnetic anomalies on the dome are likely the results of variation in the remanent magnetization of the rocks rather than induced magnetic effects.

MODEL

A single magnetic profile provides few data on which to base an unambiguous interpretation. However, due to volcanic activity on the dome it proved impossible to reoccupy these magnetic stations and extend the survey, as has been possible subsequently elsewhere on the dome (Connor et al., 1992). Nonetheless, the position of the survey relative to the subsequent extrusion of the new dome lobe, and the robust character of the anomaly, suggest that modeling is warranted. Numerous three-dimensional models were calculated in order to estimate source geometries creating the short-wavelength, large amplitude magnetic
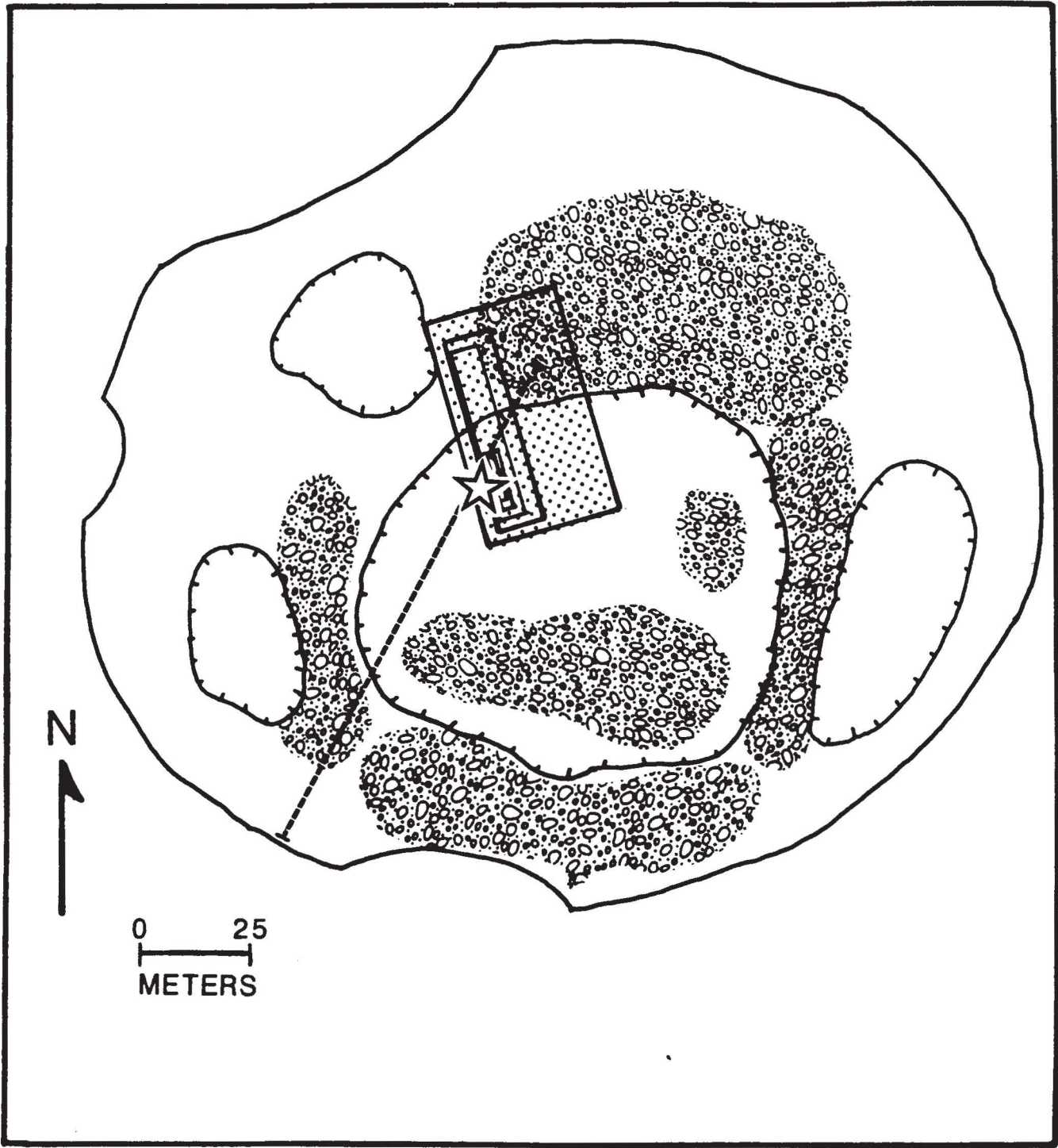
Fig. 3. Location of the ground magnetic traverse (heavy dashed line). The magnetic model (shaded area) is superimposed to facilitate comparison to other dome features (see text). In map view the model consists of five nested boxes. Each box in the model represents a volume of rock heated above the Curie-point isotherm. The top of the innermost, smallest box is at a depth of 5 m. Larger boxes are located at successively greater depths (also see Figures 4a, 4b and 6). Other symbols and map patterns are as in Figure 1.

anomaly over the active fumarole field (Plouff, 1976). We incorporated several constraining geologic features into the magnetic model. The summit dome entirely fills the summit crater. The surface of the dome consists of large boulders and talus of highly variable size and shape. Some parts of the dome are covered with a thin veneer of pyro-

clastic and epiclastic material. Most of the talus has likely moved since cooling through magnetic blocking temperatures, leading one to expect randomly oriented remanent magnetization vectors associated with individual boulders. The net result should be many short wavelength magnetic anomalies. Beneath this talus, probably at a depth of five to

Table 2

Magnetic properties of representative Volcán Colima specimens

Sample identification	NRM (A/m)	Susceptibility (mass corrected SI)
CO16-C	2.75	2.61×10^{-5}
CO18-1B	3.25	4.75×10^{-5}
CO18-2B	1.08	7.83×10^{-5}
CO18-3D	3.66	6.76×10^{-5}
CO18-4B2	3.19	8.16×10^{-5}
CO18-6C	3.84	5.66×10^{-5}

NRM is the normal remanent magnetization. All values were measured at room temperature prior to treatment.

ten meters based on observations at other domes (Rose *et al.*, 1970; Dzurisin *et al.*, 1990) and blocky lava flows (eg: Borgia *et al.*, 1983), rocks have not rotated significantly since they cooling slowly through blocking temperatures. Therefore we expect the magnetic field over the dome to be dominated by the uniformly magnetized and more indurated dome interior with little contribution (other than short wavelength noise) from surface rocks which form a carapace over this indurated core (Dzurisin *et al.*, 1990).

Based on the coincidence of high temperature fumaroles and the negative anomaly, we anticipated a thermal origin for the anomaly. Rocks heated through their magnetic unblocking temperatures become demagnetized and a remanent magnetization contrast is created between these hot rocks and cooler dome rocks surrounding them. Variation in the magnetic mineral fraction between individual flows occurs but is overwhelmed by thermal variations.

Elevation change along the traverse was not measured, but total elevation change along the traverse was estimated to be less than 20 m. Small, but deep pit craters and rubbly dome lobes along the southern half of the profile are likely responsible for spikes in the observed data in that area. The long wavelength topography of the summit dome itself also produces a magnetic effect, assuming it is uniformly magnetized (Nishida and Miyajima, 1984). Calculations suggest that these topographic effects could create long wavelength magnetic anomalies along the traverse of no more than 300nT. Because this value is small compared to the observed anomaly, no attempt was made to apply this terrain correction to the observed data.

A representative set of magnetic models are illustrated in Figures 4a and 4b. Because of the large amplitude and short wavelength of the negative anomaly near the fumarole field, all the models fitting the observed data had a very shallow source and a very low magnetic susceptibility and very low intensity of remanent magnetization, representing a body of hot, essentially non-magnetic rock. Therefore, remanent magnetization contrast between the

hot body and surrounding rocks is 4.0 A/m, a contrast deduced from rock magnetic experiments. A total magnetization vector is calculated using measured susceptibility and the Earth's field strength (0.41 Oe), but induced susceptibility is small compared to remanent magnetization, and the total magnetization vector is due almost entirely to remanent effects. The model is also very sensitive to the orientation and depth of this body. All models showed that the source geometry must be elongated in a NNW direction, oblique to the trend of the magnetic traverse, and must widen considerably with depth (Figure 4a). At its shallowest point, this body is approximately one meter wide at a depth of 5 m and widens to approximately 30 m at a depth of 50 m. Model results are strongly influenced by changes in the width, and to a lesser extent, the length, of the body at depths less than 50 m.

In Figures 4a and 4b, the body maintains a constant width and length from a depth of 50 m to the modeling depth of 100 m. The model calculations are not changed significantly by increasing the width of the body by up to 10 m at a depth of greater than 75 m. We believe this body represents a volume of rock in, and adjacent to, the high temperature fumarole field which has been heated above unblocking temperatures. Variation in depth to the top of the body, therefore, represent change in depth to the Curie-point isotherm. It makes sense that a comparatively small volume of rock was heated above this temperature, approximately 8.4×10^4 m³, in light of the limited area of high temperature fumaroles mapped at the surface and the lack of magmatic activity for nearly six years preceding this survey.

This source body cannot, however, account for the steep magnetic gradients found south of the fumarole field. The traverse crosses several rubbly dome lobes and pit crater in this area. A second body was added (Figure 4b) to account for these steep gradients. This body has a slightly lower remanent magnetization (3.1 A/m) than the dome rocks located to the north, and could represent either a thickening of the carapace on this part of the dome, or simply a lower intensity of magnetization in these dome rocks. It is possible to vary the geometry a great deal, and still adequately model the magnetic data. However, the body must be shallow, broad, and have a small magnetization contrast with other dome rocks, unlikely the source body associated with the fumarole field.

NUMERICAL MODEL FOR HEAT TRANSFER IN THE 1990 FUMAROLE FIELD.

Analysis of the fumarole temperature and ground magnetic data suggests that fumaroles in this area were degassing in a steady-state during 1990. Heat is lost from the fumarole gas as it ascends at relatively low velocities and dome rocks surrounding the fumaroles are heated. Fumarole temperatures, and the volume of rock heated about the fumarole field, depend on mass flow because the gas loses heat to wall rock as it rises. The amount of heat lost from the gas depends on the temperatures of the wall rock, the
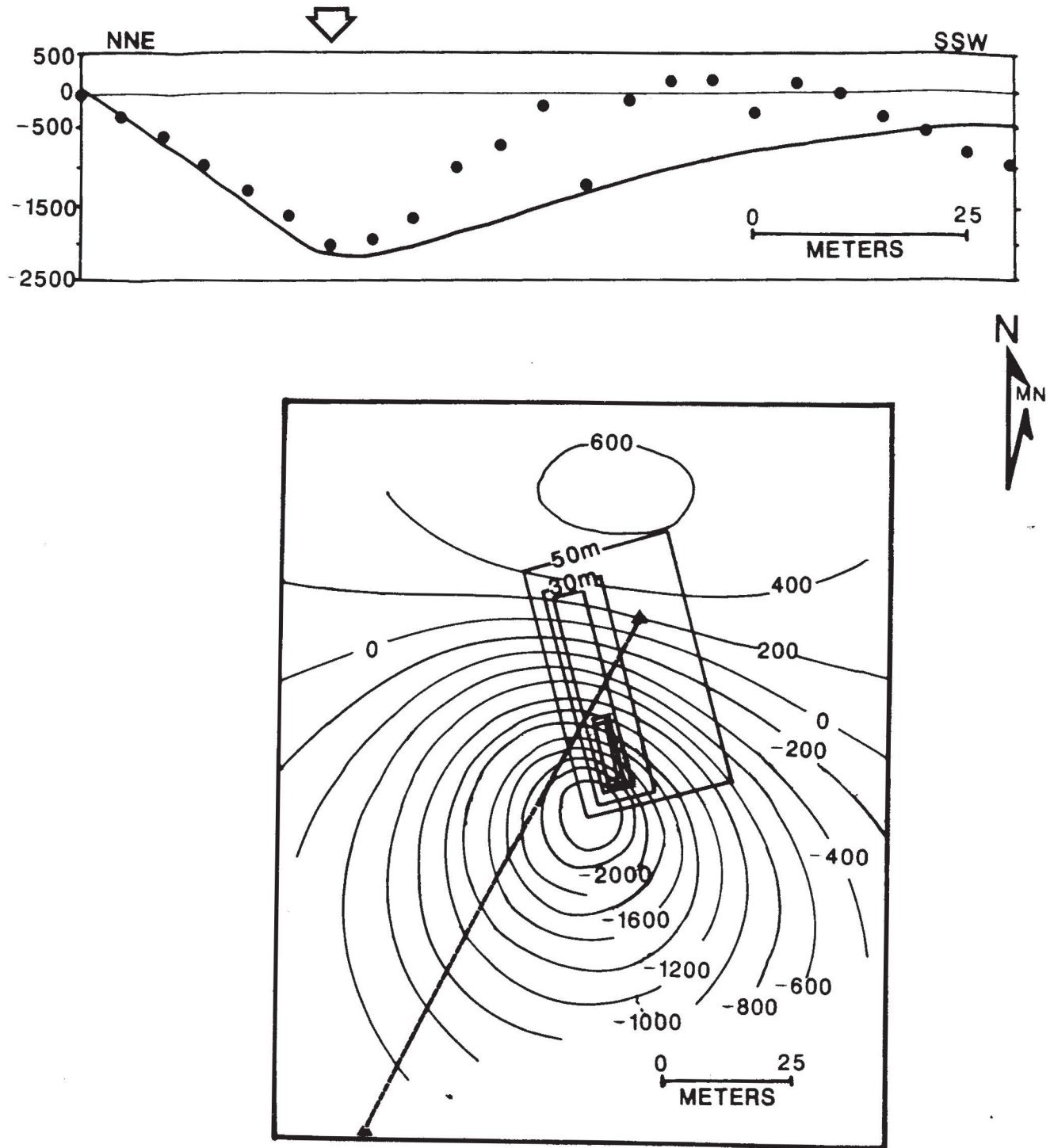
Fig. 4a. Observed, drift-corrected magnetic data (solid dots) and calculated model curve (solid curve) for the source geometry illustrated. The model consists of a series of superimposed boxes which extend from varying depths downward to a modelling depth of 100 m. From the smallest, innermost box outward, the depth from the surface to the top of each box is: 5 m, 10 m, 18 m, 30 m and 50 m, respectively. A calculated magnetic anomaly map (contour interval, 200 nT), and the location of the traverse (dashed line) are superimposed on the model. The model source body consists of hot, essentially non-magnetic rock surrounded by cooler dome rock (susceptibility = 4.23×10⁻⁵ mass-corrected SI, remanent magnetization = 4.0 A/m) (Table 2). This calculated magnetic anomaly accounts well for the magnetic gradient north of the fumarole field (indicated on the profile by the arrow) and the amplitude of the anomaly, but not for observations made south of the field.
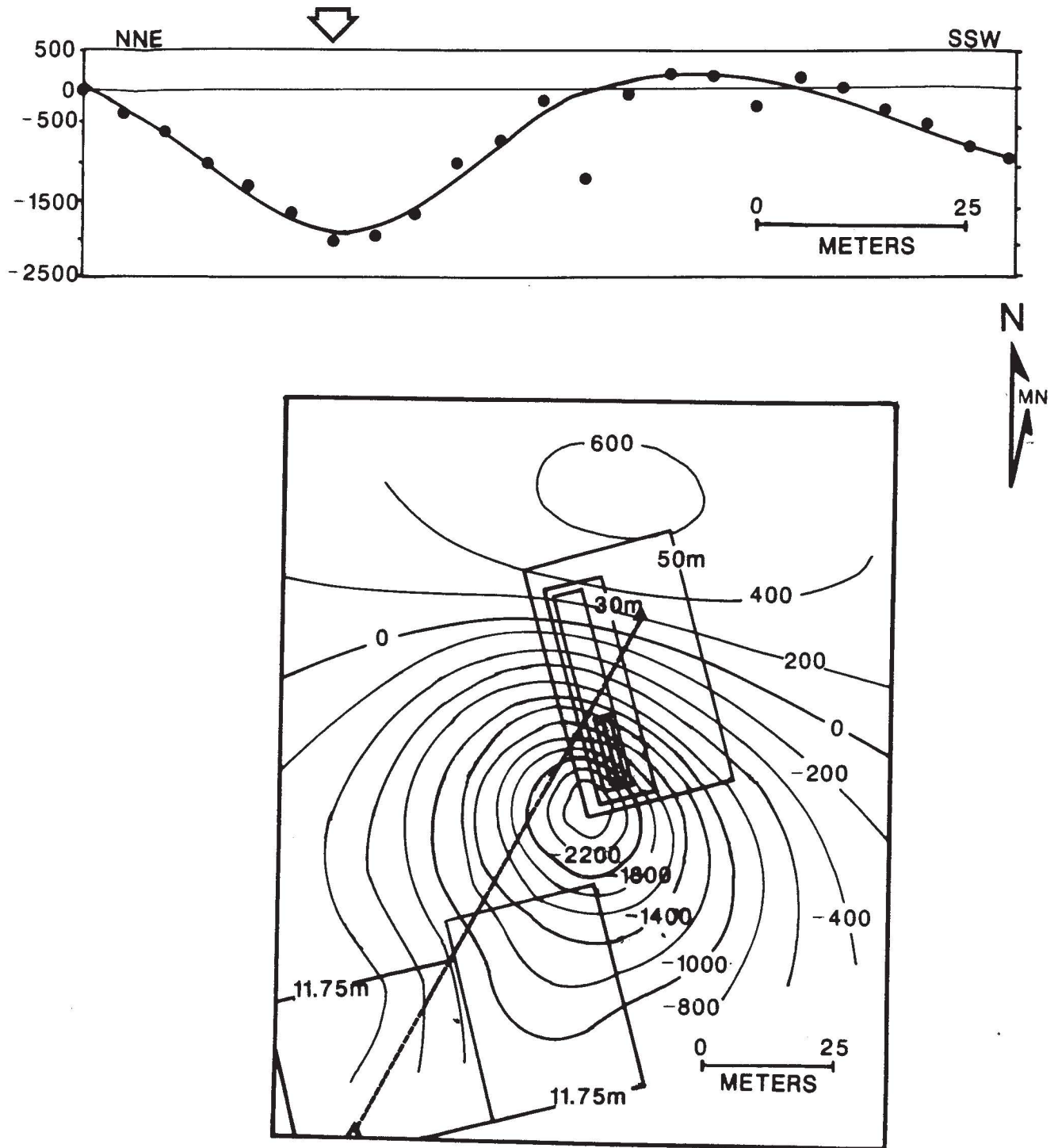
Fig. 4b. Adding a thin, shallow body with a slightly lower intensity of remanent magnetization (3.1 A/m) than other dome rocks increases the magnetic gradient south of the fumarole field, resulting in a better fit to the observed data. Some variation in the size of this body and the magnetization contrast between this body and the rest of the dome is possible, while retaining good fit to the observed data. Other aspects of the model and map features are as in Figure 4a.

length and geometry of the fumarole conduit, and the velocity with which gas is flowing. In a steady-state, gas will lose heat at a rate high enough to maintain a thermal boundary layer in the dome rock, within which rock temperatures will be elevated. As a result, gas temperature decreases in a nonlinear fashion as the gas rises. We developed a numerical heat and mass transfer model to more fully assess the relationship between fumarole temperature, mass flow, and the thickness of this thermal boundary layer. Specifically, we use the heat transfer model to evaluate the likelihood that degassing at low mass flow and high temperature could generate a thermal anomaly similar to that deduced from the magnetic model.

Numerical methods for modeling heat and mass transfer in fumaroles and hot springs have been described by Sorey (1978) and Connor (1990; 1991). Here, a fracture geometry is used because the high-temperature fumaroles appear to be fracture controlled. It is assumed that the initial gas temperature at the base of the fracture is about 800°C. Surface rock temperature is also taken to be constant far from the fumarole. Far from the fracture a constant geothermal gradient is maintained and, except in the fumarole itself, heat is transferred through the rock by conduction. The fracture is approximated as a parallel-sided conduit of constant width and hydraulic diameter, D_h. Assuming the fracture is long relative to its width, D_h is equal to twice the fracture width (Chapman, 1984).

The fumarole gas is assumed to have the thermodynamic properties of steam. Under these circumstances, flow in the frature is laminar (Reynolds number, Re < 2,200) for the ranges of fracture width and gas velocity considered here. In the laminar flow regime the Nusselt number is held constant; Nu = 8.66 for a long parallel-sided fracture. The average heat transfer coefficient can then be calculated:

$$h = \frac{Nu \cdot c}{D_h} \quad (1)$$

where c is the thermal conductivity of the gas. The gas temperature at the exit of a short segment of fracture can be expressed in terms of gas temperature at the entrance of the segment, T_{en}, average wall temperature along the length of the short segment, T_w, gas heat capacity, cp, heat transfer coefficient, h, conduit segment length, dL, fracture width, a, gas density, ρ, and velocity, v:

$$T_{ex} = (T_{en} - T_w)e^{\left(\frac{-2hdL}{v\rho acp}\right)} + T_w \quad (2)$$

The average gas temperature within the conduit is:

$$T_{avg} = exp\left(\frac{ln(T_{ex}) + ln(T_{en})}{2}\right) \quad (3)$$

A problem arises because the thermodynamic properties of the gas vary significantly as a function of temperature. Therefore, an iterative solution is required to calculate the exit gas temperature, T_{ex} in each vertical segment of the fracture. The iteration continues until T_{ex} changes by less

than 0.25°C between successive calculations. Then, T_{ex} of one fracture segment is used as the T_{en} of the next, higher (nearer surface) fracture segment. Fracture segments must be short enough so that the thermodynamic properties of the gas, calculated using T_{avg}, and wall temperature, T_w, do not vary significantly along them. Here, a segment length, dL, of 1 m is used, because mass flows are low. Applying these procedures, the gas temperature and heat transfer coefficient are determined for the fracture, given a known wall temperature gradient.

In the steady-state, the new temperature profile near the fumarole is calculated by a finite difference approximation of LaPlace's equation (eg: White, 1988). As boundary conditions, surface temperature and the temperature at the base of the fracture are assumed to be constant. Far from the fumarole $\partial T/\partial x$ is assumed to be constant, where x is distance from the fracture and convective boundary conditions are assumed to exist along the wall of the fumarole itself (White, 1988).

Once the new steady-state geothermal gradient is calculated, gas temperatures are recalculated using the new set of T_x. Gas temperatures and wall temperatures are calculated repeatedly until the solution converges and gas temperatures along the conduit remain constant between successive iterations. The resulting fumarole temperature and distribution isotherms within the surrounding rock can then be determined.

Several solutions were calculated for low mass flow rates in an attempt to illustrate the thermal structure of the 1990 fumarole field. One such solution is given in Figure 6. The essential features of this model are a low mass flow (gas velocities of 1 m/s or less), a thin fracture (5-15 cm in width), and a shallow fracture depth. A local geothermal gradient of 200°C/100 m is assumed for the summit dome. In the model, magmatic temperatures (800°C) are restricted to a zone 100 m beneath the fumarole field. Gas enters the conduit at a depth of 100 m and at a temperature of 800°C. By the time the gas exits the conduit at the surface it has cooled to 520°C. If dome rocks around the fumarole are heated purely by conduction, steeply dipping isotherms, such as those illustrated in Figure 6 will develop. In this case the Curie-point isotherm, 550°C-580°C for Colima dome rocks, will vary in distance from the fracture. At shallow depths, it will be located 5-10 m from the fracture. At depths greater than 50 m, this distance increases from 10 m to 35 m. Super imposing the magnetic model (Figures 4a and 4b) on the heat transfer model (Figure 6) demonstrates that there is good agreement between the two solutions. In other words, a volume of rock similar to that estimated by the magnetic model is likely to be heated above the Curie-point temperature of magnetite, by fumaroles degassing at a steady, low mass flow rate from a shallow source.

STRUCTURE OF THE MARCH, 1991 DOME LOBE

Dramatic changes accompanied the inital extrusion of the 1991 dome lobe, including: the formation of a graben
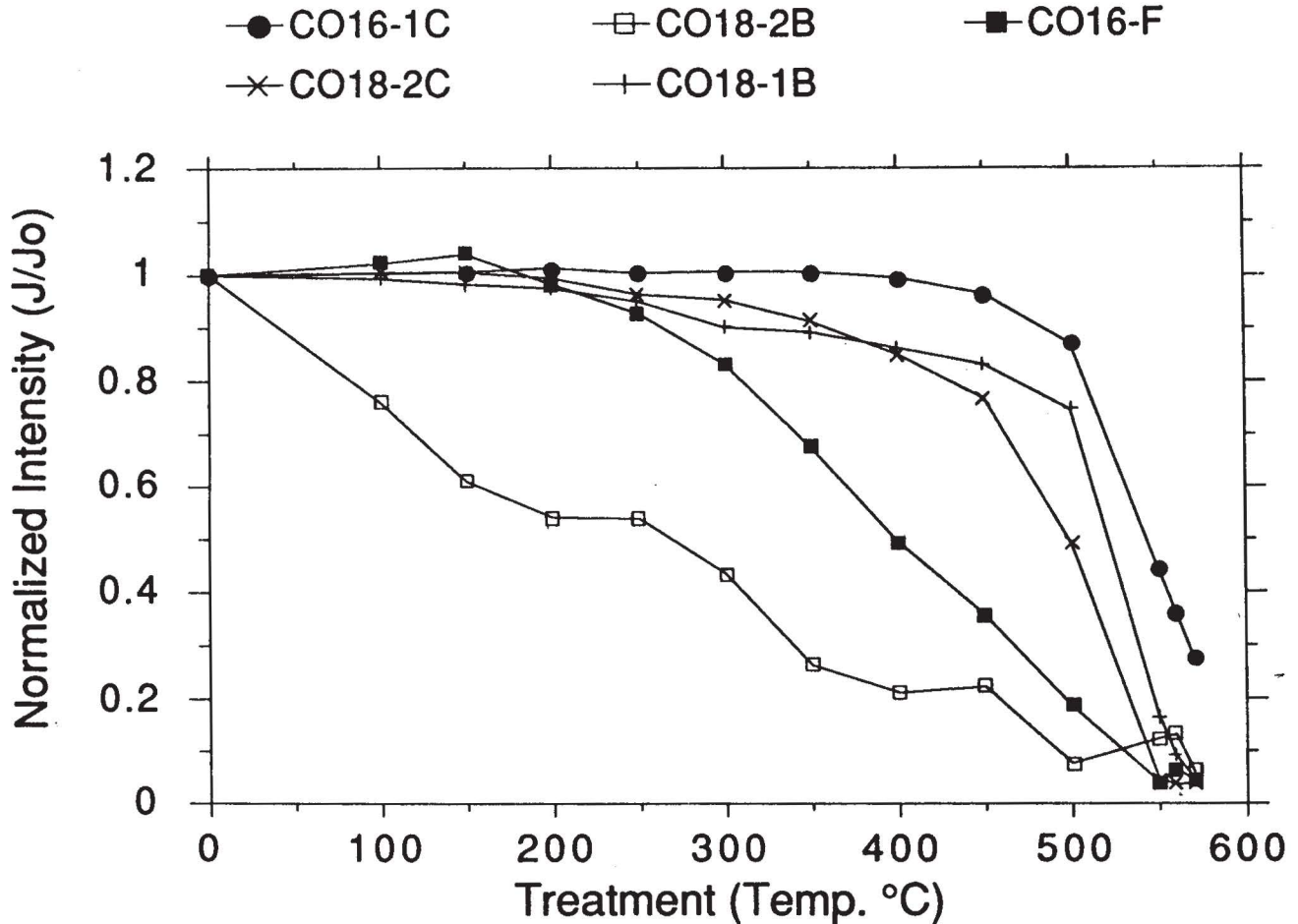
Fig. 5. Thermal demagnetization curves for selected specimens from the summit dome of Volcán Colima. All samples were collected at the surface of the dome. These curves illustrate the range in unblocking temperatures for all of the specimens.

and radial fractures that are symmetrical about the extrusion, widespread rock avalanching, and episodes of intense degassing (Figure 7). Extrusion was preceded by two seismic swarms, the first occurring during 14 February-16 February, and the second during 23 February-2 March. Each of these swarms consisted of hundreds of A and B -type earthquakes and was accompanied by increased degassing (GVN, 1991).

The new dome lobe was first observed from the air on March 1 (daily overflights of the summit crater began on 27 February). Field measurements were made of the dome lobe on March 2. The new dome lobe was roughly circular, and measured approximately 20 m in diameter and 6.5 m in height. Only the uppermost 1.5 m of the dome consisted of juvenile material. The lower 5 m consisted of older dome material that had bulged upward. Total erupted volume at this time was approximately 2000 m³, assuming that only a thin veneer of older summit dome rubble covered extrusive material on the lower flanks of the dome lobe. A shallow moat, 2-3 m deep and approximately 5 m wide surrounded the dome lobe, giving it the classic morphology of an exogenous dome (Figure 7; Williams and McBirney, 1979). Degassing was intermittent and was concentrated in the moat area, rather than on the dome lobe itself. No fractures and little fumarolic alteration was evident on the dome lobe at that time. In this respect the dome lobe was very similar in appearance and size to dome lobes extruded on Santiaguito Dome, Guatemala, during episodes of effusive activity (Rose *et al.*, 1970).

New fractures were mapped using tape and compass techniques on the surrounding, older summit dome during fieldwork on 26 February, prior to the extrusion of the new dome lobe, and again on 2 March (Figure 7). Oblique airphotos taken on 2 March and 3 March were also used to map fracture distribution. Fractures were concentrated in the western half of the summit area and were generally radial to the newly extruded dome material. Most prominent among these features was a new graben trending with an azimuth of 340-355° from the dome lobe. This graben measured 22 m wide near its northern end and decreased in width toward the dome lobe itself. The walls of this graben had a maximum throw of 4.5 m, and more generally a throw of 2-3 m. Fractures in the uneven floor of the graben were open to depths of 2-3 m and were commonly 1-2 m wide. In contrast, a graben which formed during the extrusion of a new dome lobe on the crater dome of Mount St.
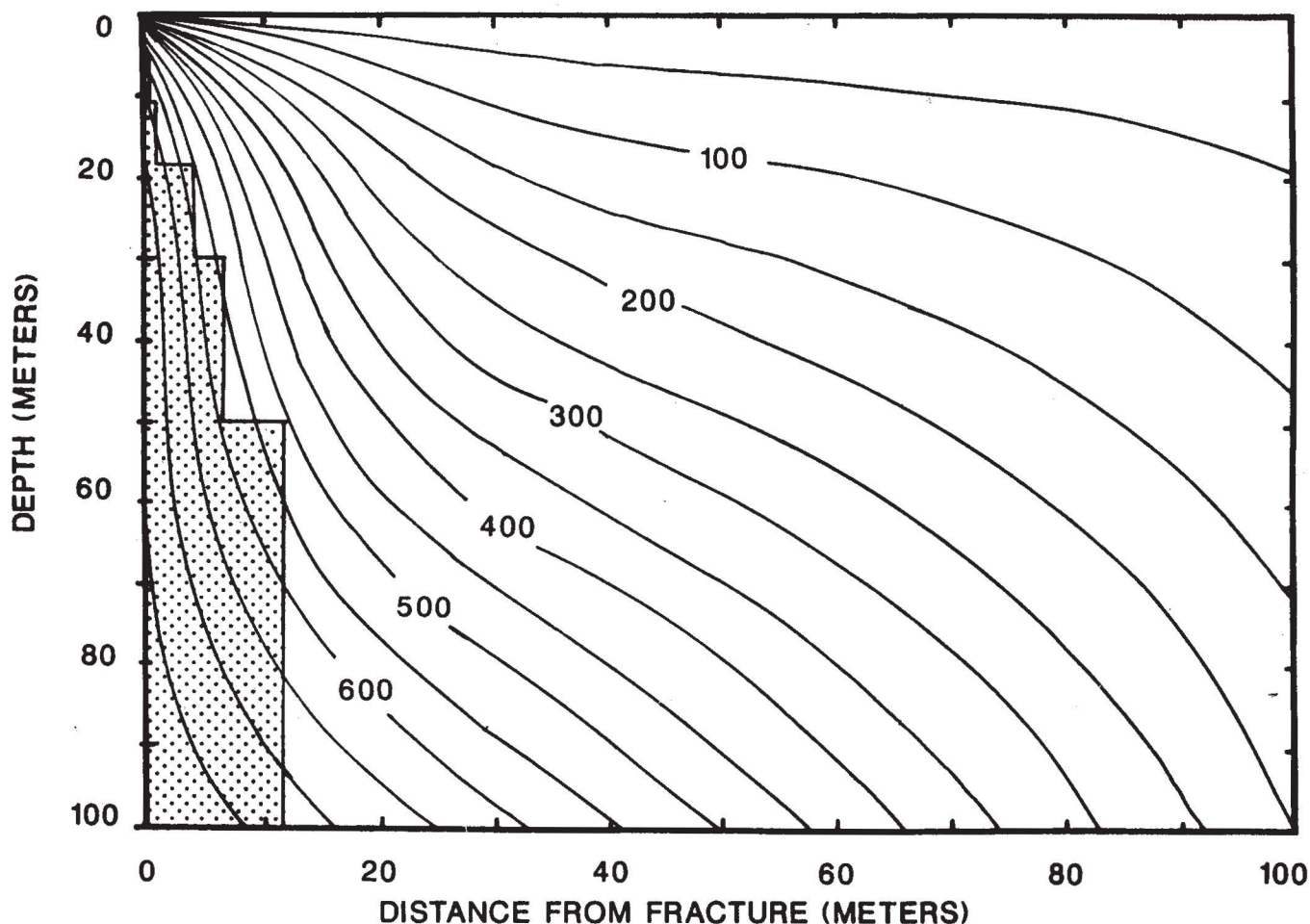
Fig. 6. One solution to the heat and mass tranfer model is illustrated. In this case, gas enters the fumarole at a temperature of 800°C at a depth of 100 m below the surface of the summit dome. The fracture width is 15 cm and the gas velocity is 1.5 m/s. The gas cools as it rises to the surface and exits the fracture at a temperature of 520°C. Heat is transferred through the wall rock by conduction, resulting in a perturbation of the local geothermal gradient. Isotherms are shown at 50°C intervals. The magnetic model (Figures 3, 4a and 4b) is superimposed on this plot (shaded area). The model is shown in cross-section, extending from the fracture westward, perpendicular to the trend of the body (Figure 3). At depths less than 75 m there is good agreement between the two models. At depths greater than 75 m a good fit to the observed magnetic data is retained even with substantial variation in the width of the magnetic model.

Helens in May, 1985 was approximately 200 m wide and about 400 m long (Dzurisin *et al.*, 1990). Curiously, fumarole activity in the graben, which formerly was the site of the highest temperature fumaroles on the summit dome, had essentially ceased (Figure 7). We were able to find only low-temperature fumaroles (< 200°C) in this area. Two other prominent fracture sets extended west and southwest of the new dome lobe. South of the new dome lobe, avalanching caused the southern rim of the summit to propagate northward toward the new dome lobe. Vertically oriented fractures were observed on this new escarpment, extending downward some 25 m from the summit area. Vertical throw rarely exceeded 1 m along these latter fracture sets.

In addition to these prominent fractures, numerous smaller fractures had opened on the west to northwest sides of the summit dome. These smaller fractures varied in width between 1 cm and 1 m, and were typically discontinuous, with overall lengths of 10 to 50 m.

Avalanche activity in late February and early March clustered on the southwest, west and northwest flanks of the volcano (Figure 1). Nearly all observed rock falls and rock avalanches (in the sense of Hansen, 1984), had source areas high on the flanks of the volcano, where slopes steepen near the summit dome. Avalanching was frequently accompanied by seismic activity (GVN,1991) and was often followed by episodes of increased degassing, suggesting a direct relationship between deformation and magma degassing at shallow levels.

DISCUSSION

Direct observations made on the summit dome prior to and immediately following the onset of extrusive activity provide insight into structural controls on this activity. Mapping of the summit dome early in March, 1991, indicates that initial seismic activity and subsequent deformation occurred in response to the intrusion of a relatively small volume of volatile-poor magma. Maximum horizontal compressional principle stresses were oriented radial to
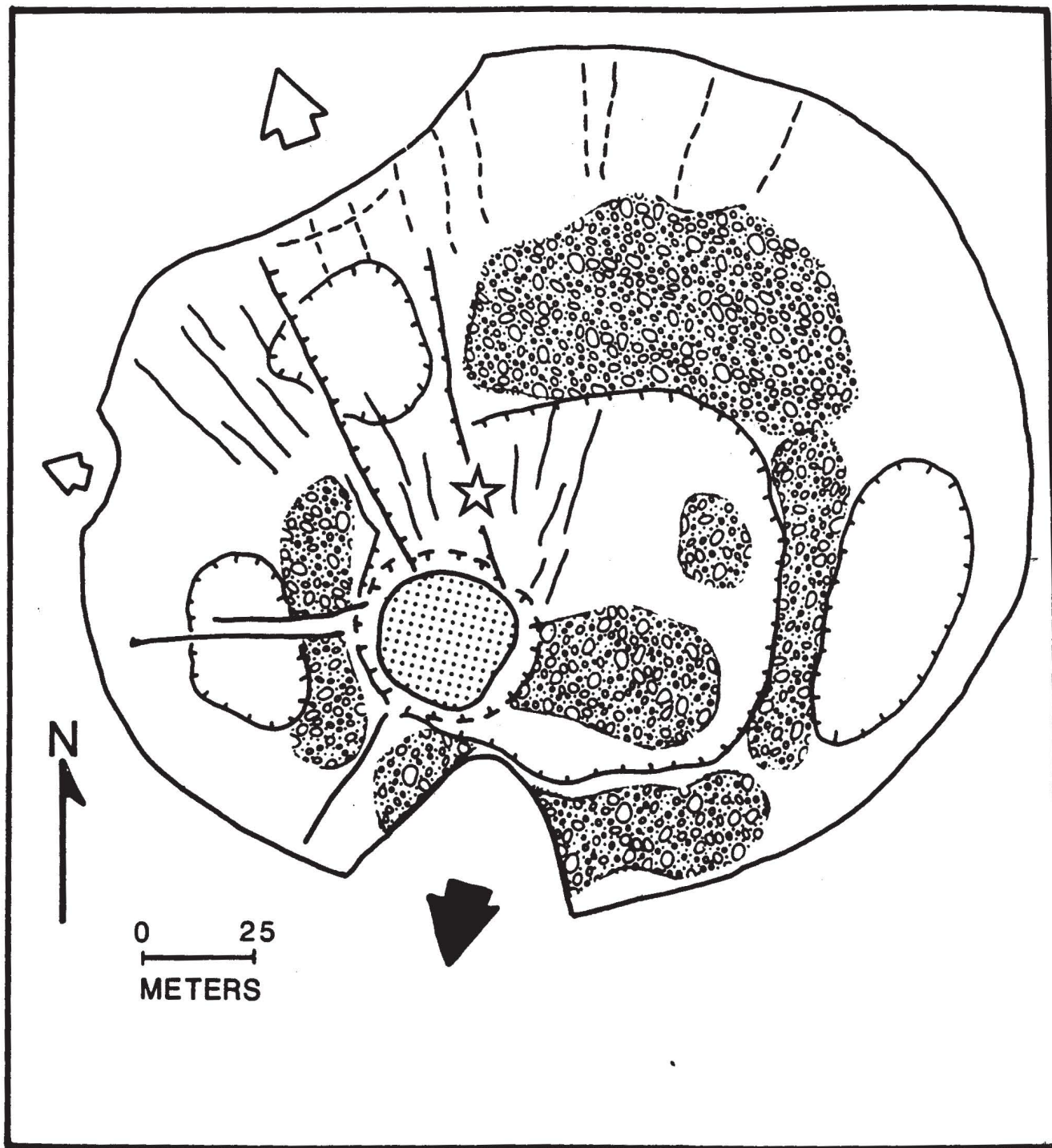
Fig. 7. Map of the summit dome of Volcán Colima prepared using field observations made on February 26, March 2 and March 3, 1991. The new lava lobe was emplaced in the south central portion of the dome (shaded), and was surrounded by a small moat (dashed hachured lines) from which degassing was intense. Prominent fractures and faults, formed just prior and during extrusion, are shown by solid lines, dashed where schematically shown. These new fractures often cut elevated rubbly areas on the older dome (pattern) and topographic depressions (hachured). Rock avalanche activity has eroded the summit dome (arrows) on the south, west and northwest. The area of high-temperature fumaroles, found on the dome prior to extrusion, is indicated (star).

the locus of extrusion and maximum horizontal extensional stresses oriented tangential to the locus of extrusion. This dome lobe extruded within 30 m of the high-temperature fumarole field we monitored throughout 1990 (Figure 7). It

seems likely, therefore, that the location of the extrusion was controlled by pre-existing structures.

An integrated approach to the interpretation of geophy-

sical anomalies helps support this observation. First, high-temperature fumaroles persisted in this area for at least one year prior to the eruption. The presence of these fumaroles indicates that mass flow was consistently higher from this area than elsewhere on the summit dome. The fumaroles were the surface manifestation of a comparatively open and permeable pathway to the surface. By comparison with temperature measurements and field observations, interpretations of the magnetic survey are limited by the paucity of the data. However, the amplitude of the observed magnetic anomaly, and the relative consistency in rock magnetic properties are supportive of a simple heat and mass transfer model. Integrating our interpretation of the magnetic data with the fumarole temperature data, through the application of the heat transfer model, indicates that fumaroles were in a steady-state, heating a relatively small volume of rock to above Curie-point temperatures over a limited area. Volatile-depleted magma, or rock near magmatic temperatures must have been located at relatively shallow depths (< 200 m) to sustain these fumaroles and their associated thermal anomaly throughout 1990, and probably long before. Finally, the magnetic model indicates that fumarole activity may have been localized along a NNW-trending fracture or fracture set, since a reasonable fit to the data is only obtained by models elongated in this orientation.

The graben that opened on the summit dome during the initial activity is a surface expression of this fracture. The largest avalanche scarps on the upper edifice are located along extensions of this graben (Figure 7). Both scarps were the sites of intense rock avalanching during 1991 activity. The southern scarp eventually became the source region of the April rock avalanche, which sent juvenile and lithic material some 4-5 km down the southern flank of the volcano (GVN, 1991; Rodríguez-Elizarraras *et al.*, 1991).

Based on these observations, we believe the NNW-trending structure, revealed by surface deformation in 1991, and manifested in geophysical anomalies in 1990, is a major structural weakness transecting the upper edifice of the volcano. It is reasonable to suspect that future activity will likely result in additional extension along this or similar structures not yet recognized. Given the hazards associated with frequent rock avalanches at this volcano, and the past occurrence of volcanic debris avalanches at Volcán Colima, it is important that direct observations of the dome continue on a regular basis.

CONCLUSIONS

The initial stage of the 1991 eruption of Colima volcano involved the effusion of a small volume of lava, resulting in the growth of an exogenous dome. Within the first 24 hours of extrusion the dome grew to a volume of about 2000 m^3. The emplacement of the dome was likely controlled, at least in part, by a pre-existing NNW-trending fracture or fracture set within the upper edifice of the volcano. Geophysical observations made on the summit dome during 1990 suggest that this structure provided a permeable conduit, through which steady-state degassing occurred long before the March, 1991 eruption.

BIBLIOGRAPHY

BAUBRON, J.-C., P. ALLARD, J.-C. SABROUX, D. TEDESCO and J.-P. TOUTAIN, 1991. Soil gas emanations as precursory indicators of volcanic eruptions, *J. Geol. Soc., London, 148*, 571-576.

BORGIA, A., S. LINNEMAN, D. SPENCER, M. L. DIEGO and J. BRENES, 1983. Dynamics of lava flow fronts, Arenal Volcano, Costa Rica, *J. Volcanol. Geotherm. Res., 19*, 303-329.

CHAPMAN, A.J., 1984. Heat Transfer, 4th ed. MacMillian Publishing Co., New York, 607 pp.

CONNOR, C. B., B. M. CLEMENT, S. B. LANE, X. SONG, G. REYES and G. ORNELAS, 1992. Continuous monitoring of an active fumarole field: Volcán Colima, Mexico. Tercera Reunión Nacional Volcán Colima, Segunda Reunión Internacional de Vulcanología, Colima, México, January 20-24, 1992, p. 6.

CONNOR, C. B., 1990. Continuous monitoring of fumarole temperatures, Colima volcano, Mexico, *EOS, Transactions of the American Geophysical Union, 71*, 43, 1694.

DZURISIN, D., R. P. DENLINGER and J. G. ROSENBAUM, 1990. Cooling rate and thermal structure determined from progressive magnetization of the dacite dome at Mount St. Helens, Washington, *J. Geophys. Res., 95*, 2763-2780.

GVN, 1990. Bulletin of the Global Volcanism Network, Smithsonian Institution, v. 15, no. 12, 2-4.

GVN, 1991. Bulletin of the Global Volcanism Network, Smithsonian Institution, v. 15, no. 12, 2-4.

HANSEN, M. J., 1984. Strategies for the classification of landslides, in (D. Brunsden and D. B. Prior, eds.). Slope Instability, John Wiley and Sons, 1-25.

LUHR, J. F., 1981. Colima: History and cyclicity of eruptions, *Volcano News, 7,* 1-3.

LUHR, J. F. and I. S. E. CARMICHAEL, 1980. The Colima volcanic complex, Mexico. I. Post-caldera andesites of Volcán Colima, *Contrib. Mineral. and Petrol., 71,* 343-372.

LUHR, J. F. and K. L. PRESTEGAARD, 1988. Caldera formation at Volcán Colima, Mexico, by a large Holocene volcanic debris avalanche. *J. Volcanol. Geotherm. Res., 35,* 335-348.

LUHR, J. F. and I. S. E. CARMICHAEL, 1990. Petrological monitoring of the cyclical eruptive activity at Volcán Colima, Mexico, *J. Volcanol. Geotherm. Res., 42,* 235-260.

MARTIN DEL POZZO, A. L., 1990. Multiple debris avalanche events in Colima, Mexico, *EOS, Transactions of the American Geophysical Union, 71,* 43, 1720.

McCLELLAND, L., T. SIMKIN, M. SUMMERS, E. NIELSEN and T. C. STIEN, 1989. Global Volcanism 1975-1985. Prentice Hall, New Jersey, 665 pp.

MEDINA, F., 1983. Analysis of the eruptive history of the Volcán de Colima, Mexico (1560-1980). *Geofís. Int., 22,* 2, 157-178.

NISHIDA, Y. and E. MIYAJIA, 1984. Subsurface structure of Usu volcano revealed by detailed magnetic survey, *J. Volcanol. Geotherm. Res., 22,* 271-285.

PLOUFF, D., 1976. Gravity and magnetic fields of polygonal prisms and application to magnetic terrain corrections. *Geophysics, 41,* 727-741.

RODRIGUEZ-ELIZARRARAS, S., C. SIEBE, J.C. KOMOROWSKI, J. M. ESPINDOLA and R. SAUCEDO. Field observations of the pristine block- and ash-flow deposits emplaced April 16-17, 1991, at Volcán Colima, Mexico, *J. Volcanol. Geotherm. Res., 48,* 399-412, 1991.

ROSE, JR. W. I., R. E. STOIBER and S. B. BONIS, 1970. Volcanic activity at Santiaguito volcano, Guatemala, June, 1968-August, 1969, *Bull. Volcanol., 34,* 295-307.

SOREY, M. L. 1978. Numerical modeling of liquid geothermal systems, U. S. Geological Survey Professional Paper 1044-D, 25p.

STOOPES, G. R., 1991. Studies of two giant debris avalanche deposits from the Colima volcanic complex, Mexico. M.S. Thesis, Arizona State University, Tempe, Arizona, 132 pp.

STOOPES, G. R. and M. F. SHERIDAN 1992. Giant debris avalanches from the Colima volcanic complex, Mexico. Implications for long-runout landslides (<100 km) and hazard assessment. *Geology, 20,* 299-302.

WHITE, F. M., 1988. Heat and Mass Transfer, Addison-Wesley Publishing Co., Reading, Ma., 718 pp.

WILLIAMS, H. and A. R. McBIRNEY, 1979. Volcanology, Freeman, Cooper, and Co., San Francisco, 379 pp.

Charles B. Connor[1], Sammantha B. Lane and Bradford M. Clement
Dept. of Geology, Florida International University, Miami, FL, 33199, USA.
[1] Current address: Center for Nuclear Waste Regulatory Analyses, Southwest Research Institute, 6220 Culebra Rd., San Antonio, Texas, 78238, USA.